# Supporting Information for

## Water absorption dependence of the formation of poly (vinyl alcohol)-iodine complex for poly (vinyl alcohol) films

Yingxu Song[1], Sumei Zhang[1], Jian Kang[1], Jinyao Chen[1,*], and Ya Cao[1]

[1] State Key Laboratory of Polymer Materials Engineering, Polymer Research Institute of Sichuan University, Sichuan University, Chengdu 610065, China.

* Corresponding author: Jinyao Chen.

E-mail: chenjinyao@scu.edu.cn. Fax: +86-28-8540-6333. Tel: +86-28-8540-6333.

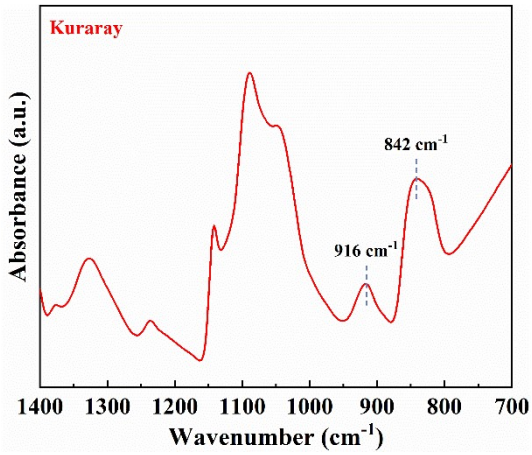


Figure S1. FTIR spectrum of PVA film provided by Kuraray Co., Ltd. (Japan).

According to the Kenney method[1], the triad tacticity was estimated by the following equation:

$$mm(\%) = -78 \times \frac{A_{916cm^{-1}}}{A_{842cm^{-1}}} + 59 \qquad \text{* MERGEFORMAT (S1)}$$

$$rr(\%) = 60 \times \frac{A_{916cm^{-1}}}{A_{842cm^{-1}}} + 7 \qquad \text{* MERGEFORMAT (S2)}$$

$$mr(\%) = 18.7 \times \frac{A_{916cm^{-1}}}{A_{842cm^{-1}}} + 34 \qquad \text{* MERGEFORMAT (S3)}$$

Because of $\frac{A_{916cm^{-1}}}{A_{842cm^{-1}}} = 0.4861$, we could calculate the triad tacticity (mm = 0.21, mr = 0.43, rr = 0.36).

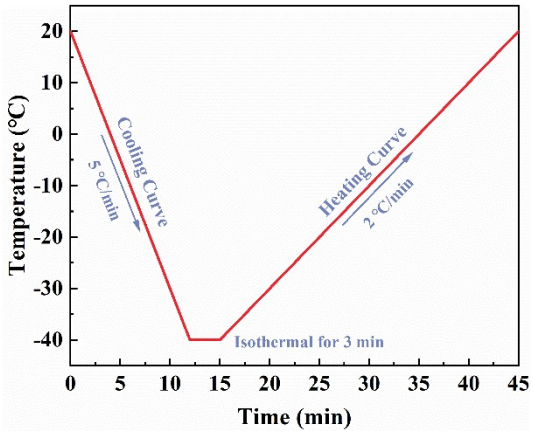


Figure S2. Program of DSC testing for determining the states of water in PVA films.

Samples with the nominal weight of 2 ~ 5 mg, were cooled from 20 ℃ to -40 ℃ at a cooling rate of 5 ℃/min, lasted 3 min at -40 ℃, and then heated to 20 ℃ at a heating rate of 2 ℃/min.

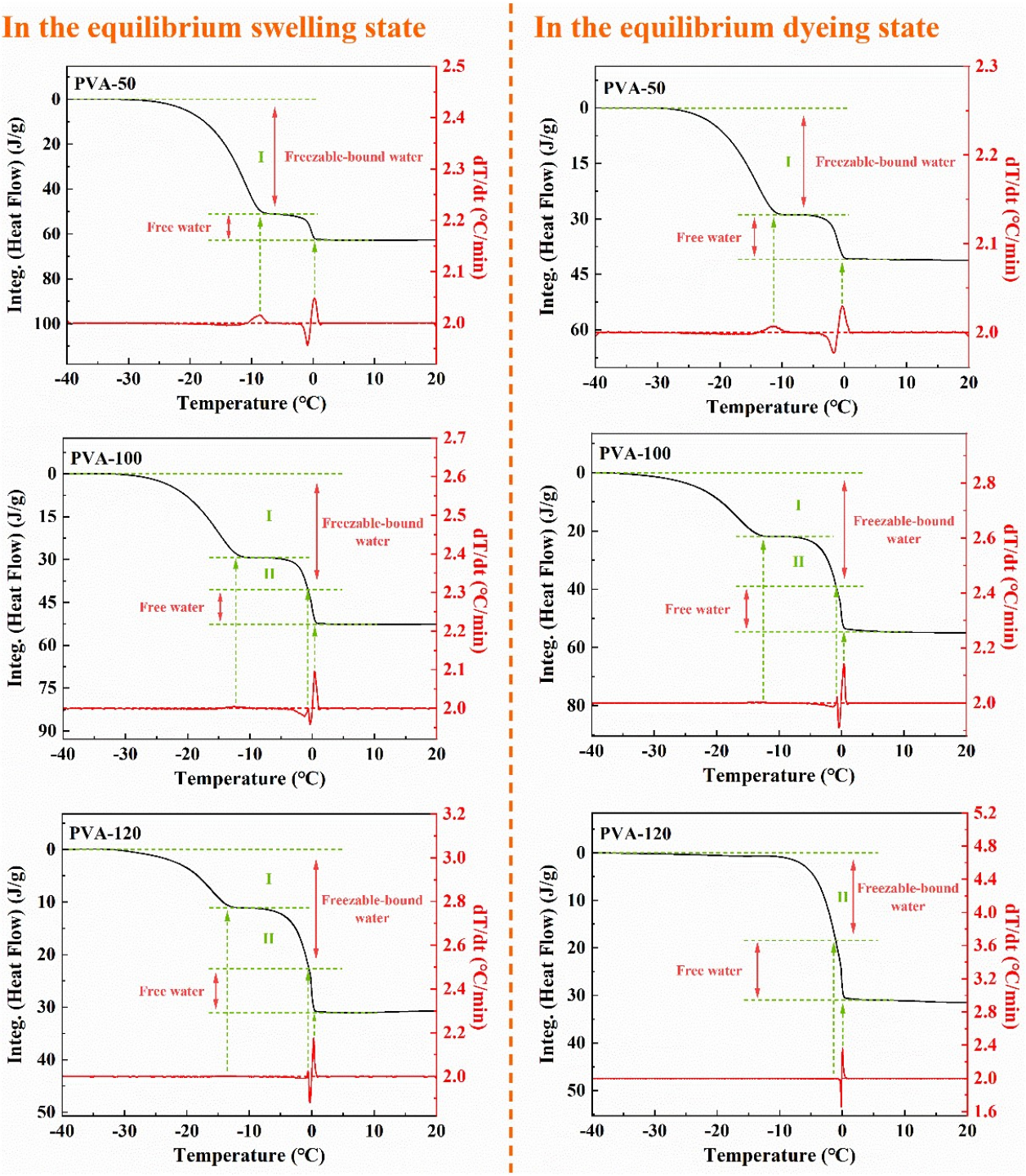


Figure S3. Subdivisions of multiple ice-melting peak areas of the equilibrium-swelling and the equilibrium-dyeing PVA samples through the variation of dT/dt based on the DSC heating curves.

The derivative of the sample temperature T as a function of the heating time t (i.e., dT/dt) deviates the programmed heating rate of 2 °C/min when the phase transition happens, and the positive dT/dt peak (> 2

℃/min) usually locates at the end of the transition, so the positive peak can be regarded as the boundary of the two adjacent phase transitions[2]. Thus, freezable bound water is divided into freezable bound water I and freezable bound water II, and the normalized enthalpies of water in different states could directly be read from the curves. Then, the ratios of the weight of absorbed water in different states to the weight of dry PVA film could be calculated quantitatively through the equations (3 - 6). All the data is shown in Table S1 and Table S2.

Table S1. The ice-melting enthalpies corresponding to different states of water for swollen PVA films.

| Swollen samples | A (%) | Peak 1 | | Peak 2 | | Peak 3 | | $w_{nfbw}$ (%) |
|---|---|---|---|---|---|---|---|---|
| | | $\Delta H_{fbw\text{-}I}$ [a] | $w_{fbw\text{-}I}$ (%) | $\Delta H_{fbw\text{-}II}$ [a] | $w_{fbw\text{-}II}$ (%) | $\Delta H_{fw}$ [a] | $w_{fw}$ (%) | |
| 50℃ | 83.24 | 51.18 | 32.49 | — | — | 11.68 | 6.42 | 44.34 |
| 100℃ | 68.67 | 29.38 | 17.16 | 11.15 | 6.52 | 12.16 | 6.15 | 38.84 |
| 120℃ | 54.97 | 11.14 | 5.98 | 11.39 | 6.11 | 8.54 | 3.97 | 38.91 |

[a] The unit of the normalized melting enthalpy is J/g swollen PVA film.

Table S2. The ice-melting enthalpies corresponding to different states of water for dyed PVA films.

| Dyed samples | A (%) | Peak 1 | | Peak 2 | | Peak 3 | | $w_{nfbw}$ (%) |
|---|---|---|---|---|---|---|---|---|
| | | $\Delta H_{fbw\text{-}I}$ [a] | $w_{fbw\text{-}I}$ (%) | $\Delta H_{fbw\text{-}II}$ [a] | $w_{fbw\text{-}II}$ (%) | $\Delta H_{fw}$ [a] | $w_{fw}$ (%) | |
| 50℃ | 82.56 | 28.88 | 18.26 | — | — | 12.02 | 6.58 | 57.72 |
| 100℃ | 68.83 | 21.99 | 12.86 | 17.30 | 10.11 | 13.30 | 6.73 | 39.13 |
| 120℃ | 54.79 | — | — | 17.91 | 9.60 | 11.88 | 5.51 | 39.68 |

[a] The unit of the normalized melting enthalpy is J/g dyed PVA film.

Table S3. The wavenumbers of all peaks and corresponding bands assignment in IR spectra.

| Wavenumber ($cm^{-1}$) | Band assignment | |
|---|---|---|
| | PVA | $H_2O$ |
| 3750 - 2950 | O-H symmetry stretching vibration | O-H symmetry stretching vibration |
| 2944, 2906 | C-H stretching vibration | / |
| 1750 - 1500 | / | O-H bending vibration |
| 1141 | crystal-sensitive band | / |
| 1046 | C-O stretching vibration | / |
| 916 | amorphous region | / |

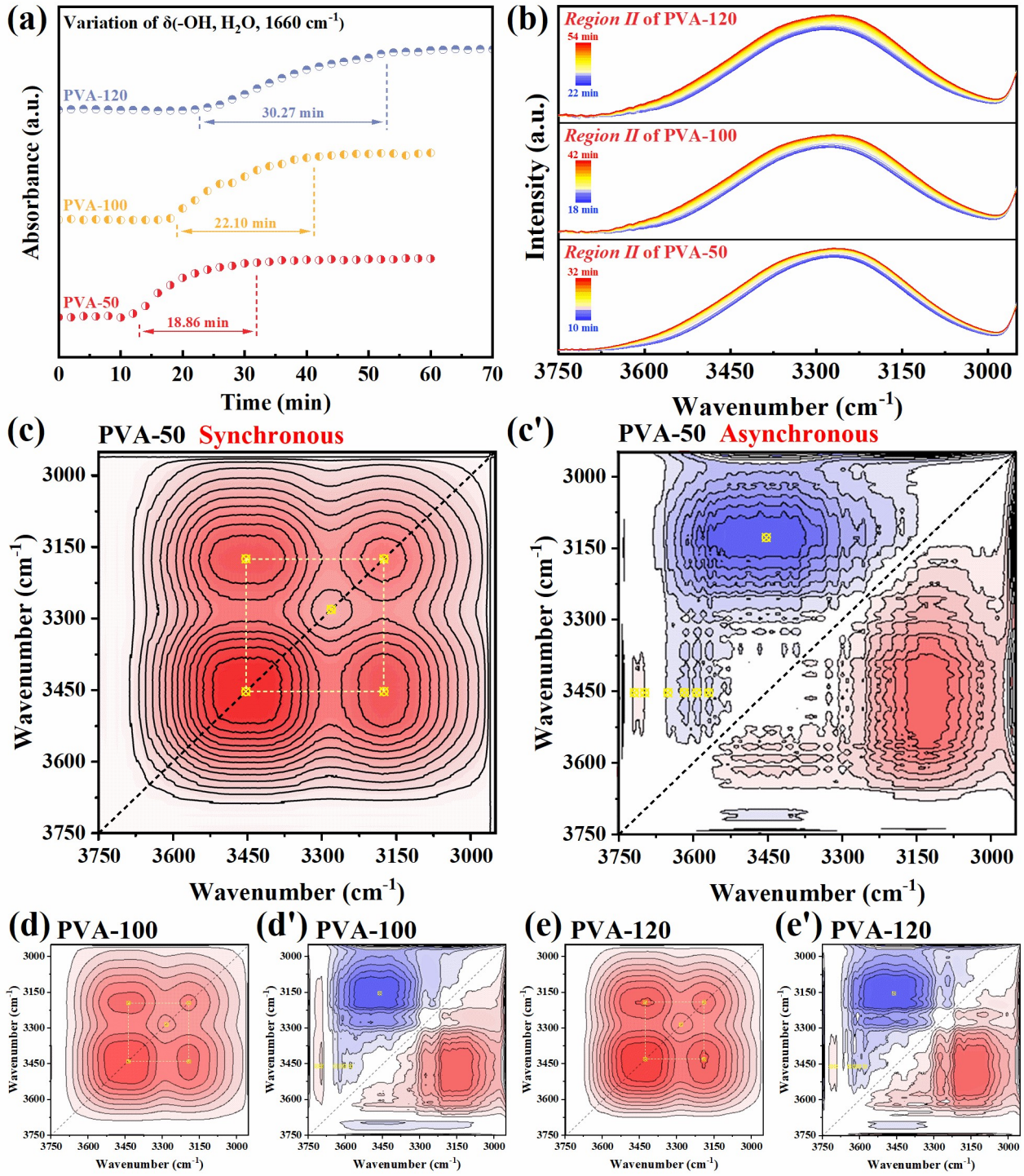


Figure S4. (a) The absorbance of δ (-OH, $H_2O$, 1660 $cm^{-1}$) as a function of diffusion time; (b) the varied spectra of Region II extracted from samples in the range of 3750 – 2950 $cm^{-1}$; (c - e) for the synchronous and (c′ – e′) for the asynchronous 2DCOS contour maps calculated from the spectra shown in (b); the red for positive peaks and the blue for negative ones.

2DCOS is an efficient tool to describe the specific responding sequence orders of characteristic bands corresponding to different structures or chemical species under the external stimulus, and absorption bands overlapped in 1D spectra are well-resolved in 2DCOS contour maps because of the enhancing resolution[3]. The range of 3750 – 2950 $cm^{-1}$ in Region II (Fig. S4a, b) was selected for the calculation of 2DCOS, and the results for the synchronous and the asynchronous are represented in Fig. S4c – e and Fig. S4c′ – e′, respectively. From the synchronous and asynchronous contour maps calculated, it's obvious that there is no distinction among different samples, indicating that the pre-annealing treatment did not change the process of water diffusion. Therefore, we choose PVA-50 as the example to describe the detailed analysis.

As shown in Fig. S4c, except for the positive cross-peak sited at φ (3453, 3175 $cm^{-1}$) in the upper left side of the diagonal line, there are also three positive auto-peaks located at 3175, 3281, and 3453 $cm^{-1}$ in the synchronous 2DCOS of PVA-50, while less information can be derived from this. Conversely, the asynchronous 2DCOS can not only distinguish compositions of the coupling bands, but also reflect the order of related bands. Five negative cross-peaks ψ ((3453, 3128 $cm^{-1}$), (3569, 3453 $cm^{-1}$), (3593, 3453 $cm^{-1}$), (3618, 3453 $cm^{-1}$), and (3651, 3453 $cm^{-1}$)) and two positive cross-peaks ψ ((3698, 3453 $cm^{-1}$) and (3719, 3453 $cm^{-1}$)) are observed in the upper left side of Fig. S4c′, which indicates that the broad peak ν (-OH, PVA + $H_2O$) in the 1D ATR-FTIR spectra is overlapped by eight single bands. Based on several previous works[4-6], we know that:

(a) 3128 $cm^{-1}$ is assigned to the $\nu_s$ (-OH, $H_2O$) of tetrahedrally coordinated water molecules with strong hydrogen bonds in bulk water;

(b) 3453 $cm^{-1}$ represents the $\nu_{as}$ (-OH, $H_2O$) of incompletely coordinated water molecules in small

water clusters;

(c) 3569, 3593, 3618, and 3651 $cm^{-1}$ are weak hydrogen bonds among water molecules or between hydroxyl groups and water molecules;

(d) both 3698 $cm^{-1}$ and 3719 $cm^{-1}$ are attributed to free water molecules with very weak or without hydrogen bonds.

Based on the Noda rules[7, 8], for synchronous cross-peak φ (ν1, ν2) and asynchronous cross-peak ψ (ν1, ν2) in the upper left side of the diagonal line, if φ (ν1, ν2) * ψ (ν1, ν2) > 0, the characteristic band at ν1 responses earlier than the one at ν2, while if φ (ν1, ν2) * ψ (ν1, ν2) < 0, the variation of band at ν1 is later than that of the one at ν2.

Thus, we conclude that the specific sequence orders of bands mentioned above is 3698, 3719 > 3128 > 3453 > 3569, 3593, 3618, and 3651 $cm^{-1}$, or (free water molecules with very weak hydrogen bonds) > (bulk water with strong hydrogen bonds) > (water clusters with incompletely coordinated water molecules) > (weak hydrogen bonds among water molecules or between hydroxyl groups and water molecules), which helps us to understand the mechanism of water diffusion into PVA matrix and draw the factors affecting the water diffusion process.

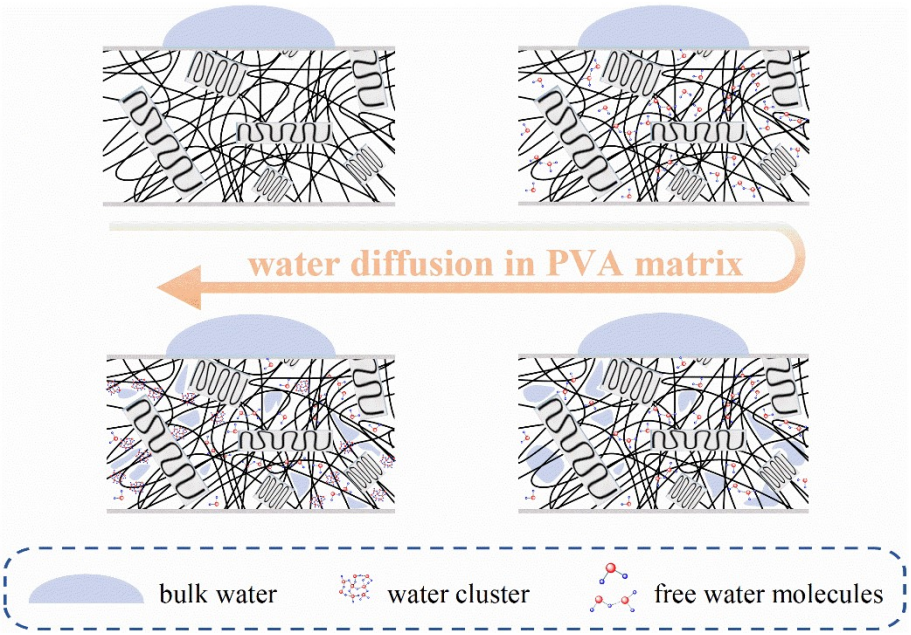


Figure S5. The schematic mechanism of water diffusion into PVA matrix.

1. Kenney, J. F.; Willcockson, G. W. Structure-Property Relationships of Poly(vinyl alcohol). III. Relationships between Stereo-regularity, Crystallinity, and Water Resistance in Poly(vinyl alcohol). *Journal of Polymer Science Part A-1: Polymer Chemistry* **1966,** 4 (3), 679-698.
2. Li, W.; Xue, F.; Cheng, R. States of water in partially swollen poly(vinyl alcohol) hydrogels. *Polymer* **2005,** 46 (25), 12026-12031.
3. Zhou, Y.; Wu, P. Block length-dependent phase transition of poly(N-isopropylacrylamide)-b-poly(2-isopropyl-2-oxazoline) diblock copolymer in water. *Polymer* **2018,** 153, 250-261.
4. Wang, M.; Wu, P. Reconsideration of the Results of the Two Dimensional Correlation Infrared Spectroscopic Study on Water Diffusion Process in Poly(ε-caprolactone) Matrix. *Polymer* **2011,** 52 (3), 769-777.
5. Peng, Y.; Wu, P.; Siesler, H. W. Two-Dimensional/ATR Infrared Correlation Spectroscopic Study on Water Diffusion in a Poly(ε-caprolactone) Matrix. *Biomacromolecules* **2003,** 4 (4), 1041-1044.
6. Sammon, C.; Mura, C.; Yarwood, J.; Everall, N.; Swart, R.; Hodge, D. FTIR-ATR Studies of the Structure and Dynamics of Water Molecules in Polymeric Matrixes. A Comparison of PET and PVC. *The Journal of Physical Chemistry B* **1998,** 102 (18), 3402-3411.
7. Noda, I.; Dowrey, A. E.; Marcott, C.; Story, G. M.; Ozaki, Y. Generalized Two-Dimensional Correlation Spectroscopy. *Applied Spectroscopy* **2000,** 54 (7), 236a-248a.
8. Zhou, T.; Zhang, A.; Zhao, C. S.; Liang, H. W.; Wu, Z. Y.; Xia, J. K. Molecular Chain Movements and Transitions of SEBS above Room Temperature Studied by Moving-Window Two-Dimensional Correlation Infrared Spectroscopy. *Macromolecules* **2007,** 40 (25), 9009-9017.